Measurement Method for Two-dimensional Normal Stress Distribution of Wheels on Lateral Loose Soil Slopes

Shoya Higa, Kenji Nagaoka, Keiji Nagatani, and Kazuya Yoshida

***Abstract*— Surfaces of exploration targets for lunar/planetary robots (rovers), such as the Moon and Mars, are covered with fine sand. This sand makes the wheels of a rover susceptible to slip, and in the worst case, can lead to immobility. To avoid such situations, it is important to analyze the mechanics of the interaction between the soil and wheel. Hence, various devices to measure the normal stress distribution beneath wheels have been proposed. However, most of the conventional equipment is only able to measure the distribution in a flat soil environment. In practice, when a rover traverses sandy slopes, the normal stress distribution is not expected to have a simple shape like that for a flat environment. Therefore, we propose a measurement device for the two-dimensional normal stress distribution of a wheel on a lateral loose soil slope. Some experimental results prove the validity of the method.**

I. Introduction

Target environments for lunar/planetary exploration robots (rovers), such as the surfaces of the Moon and Mars, are covered with fine and loose sand. Wheel slippage occurs easily, making it difficult for a rover to follow a given path. In the worst case, wheels can become buried in the sand and the robot can become immobile. To avoid such situations, several studies have been conducted, based on the mechanics of the interaction between a wheel and soil [1], [2], [3].

In this research field, called terramechanics, a rover's weight and generated drawbar-pull are calculated by using the normal stress and shear stress distributions beneath its wheels. Therefore, knowing the actual stress distribution in detail is very useful to validate a wheel-soil interaction model. Thus, measurements of the stress distributions generated beneath a wheel have been conducted using various measurement devices [4], [5], [6], [7], [8].

Hegedus [4] used three transducers per wheel width. Krick [5] and Senatore et al. [7] used five cantilevers with strain gage per half wheel width. Nagatani et al. [6] used built-in pressure sensor array that have four pressure sensors per wheel width. Shirai et al. [8] used an in-wheel sensor system that included eight pressure sensors and light sensors. This system detects contact area accurately, but have two pressure sensors per wheel width. These devices that used for stress distribution measurements have low resolution or do not cover the whole wheel width. Almost all of the typical measurements have only been conducted on flat and loose soil.

On the other hand, future exploration missions using rovers on the surface of the Moon and Mars will require traversing more challenging terrains such as a steep slope in the inner portion of a crater. Our research group has conducted lateral traversability analyses of a rover on steep slopes. In this research, we confirmed that the path tracking ability is improved by changing the contact angle of the wheels, and theoretically verified the reason for the improvement [9]. However, in the above research, the actual stress distribution generated beneath a wheel was not measured directly. Therefore, in this paper, we propose a method for precisely measuring the stress distribution generated beneath a wheel when a rover laterally traverses a sandy slope.

S. Higa, K. Nagaoka, K. Nagatani, and K. Yoshida are with Graduate School of Engineering, Tohoku University, 6-6-01 Aoba Aramaki Aoba-ku, Sendai 9808579, Japan {shoya,nagaoka,keiji,yoshida}@astro.mech.tohoku.ac.jp

Fig. 1. A Traversal Situation of a Wheeled Robot

In section II, we explain the two-dimensional (2D) stress distribution measurement system developed in this paper. In section IV, we report the results of a measurement experiment for the 2D stress distribution generated beneath a wheel when a rover traverses a loose soil slope. Finally, in section V, we discuss the validity of the experimental results.

II. Experimental Setup

We target a wheeled rover that traverses a sandy slope laterally, and the rotational axes of the wheels are perpendicular to the gravity direction as shown in Fig. 1. In this case, the sinkage depth at the each side of a wheel will be different. Thus, it is expected that the shape of the stress distribution generated beneath the wheel in the above case will be different from that on flat terrain. Therefore, our objective is to obtain the stress distribution beneath a wheel in the above case.

In this section, we introduce our measurement equipment, a target experimental environment, and our measurement method.

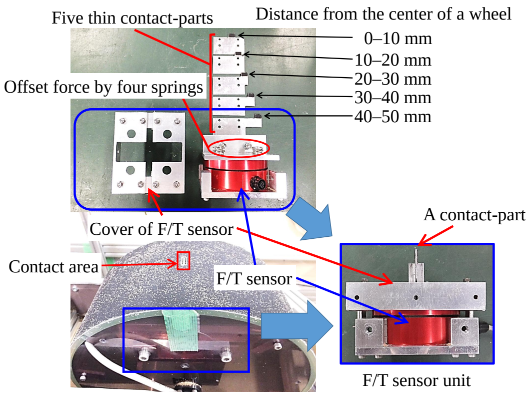

Fig. 2. F/T Sensor Unit (F/T Sensor + Contact-parts)

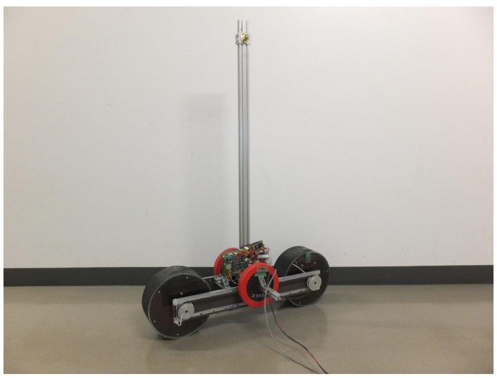

Fig. 3. Two-wheel Rover Test Bed

A. Measurement Equipment

In this study, a force/torque (F/T) sensor unit was developed as a measurement device. The unit contains a 6-axis F/T sensor and five "contact-parts" made of thin aluminum plates, as shown in Fig. 2. These contact-parts fit through holes in the wheel surface on one end a interface with the F/T sensor on the other. Each contact-part is a different shape to allow for measurements at different distance from the center of the wheel. These distances between the contact-part positions and the center of the wheel are 0–10 mm, 10–20 mm, 20–30 mm, and 40–50 mm. The contact area of each contact-part is 2.4 mm $\times$ 10.4 mm. By using the five types of contact-parts, the stress distribution in a wheel's circumferential direction can be measured at a total of 10 positions. Moreover, four springs are attached to the surface of the 6-axis F/T sensor to always generate an offset force. Based on these mechanisms, the dead zone of the 6-axis F/T sensor is outside the measurement range.

In this study, the F/T sensor unit is mounted on the rear wheel of two-wheel rover test bed (Fig. 3). By using this unit, the stress distribution corresponding to the rotational angle of the wheel can be measured by rotating the wheel on loose soil. Table I shows the specifications of the rover test bed.

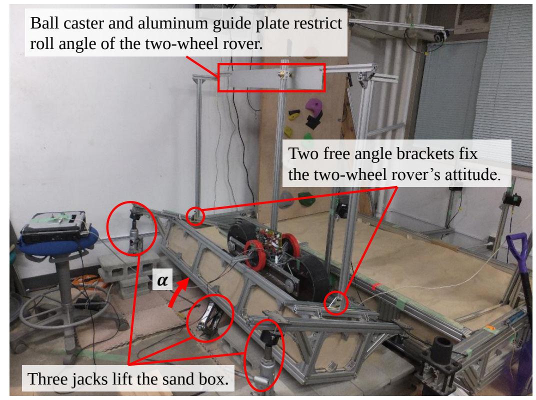

Fig. 4. Experimental Environment

B. Experimental Environment

As shown in Fig. 4, a sandbox, which is 1.6 m in length, 0.3 m in width, and 0.2 m in height, is used for our target environment. It can be used to form a loose soil slope of up to approximately 20°. The inclination angle α is generated by lifting one side using three hydraulic jacks. In addition, in order to maintain the attitude of a wheel, a 1-m-long pole is mounted on the two-wheel rover test bed body, and two ball casters are mounted at the top of this pole. The attitude is supported by the ball casters and aluminum guide plate. Note that this aluminum guide plate can be fixed at any tilt angle by considering the slip angle of the rover. Thus, it is possible to measure the stress distribution generated beneath a wheel while maintaining a constant attitude for the two-wheel rover. The sandbox is filled with Toyoura standard sand. The particle diameters of the sand are nearly homogeneous, and its cohesion is nearly zero. The soil was raked and smoothed before the stress distribution generated beneath a wheel is measured.

C. Measurement Method

The 2D stress distribution of a wheel is measured using the following procedure:

1. Incline the sandbox to any inclination angle α, using three hydraulic jacks.
2. Attach a contact-part to 6-axis F/T sensor, and mount the F/T sensor unit in the rear wheel as shown in Fig. 2.
3. Incline the aluminum guide plate to set the bottom of the robot perpendicular to the gravity direction.
4. Rake the soil to ensure a flat sand surface.
5. Traverse the two-wheel rover test bed and adjust the yaw angle of the aluminum guide plate.
6. Repeat steps 4 and 5, and perform micro-adjustments to the attitude of the two-wheel rover.

TABLE I
SPECIFICATIONS OF TWO-WHEEL ROVER

Size [mm]	L830 $\times$ W520 $\times$ H1190
Mass [kg]	14.8
Wheel size [mm]	ϕ250 $\times$ W100

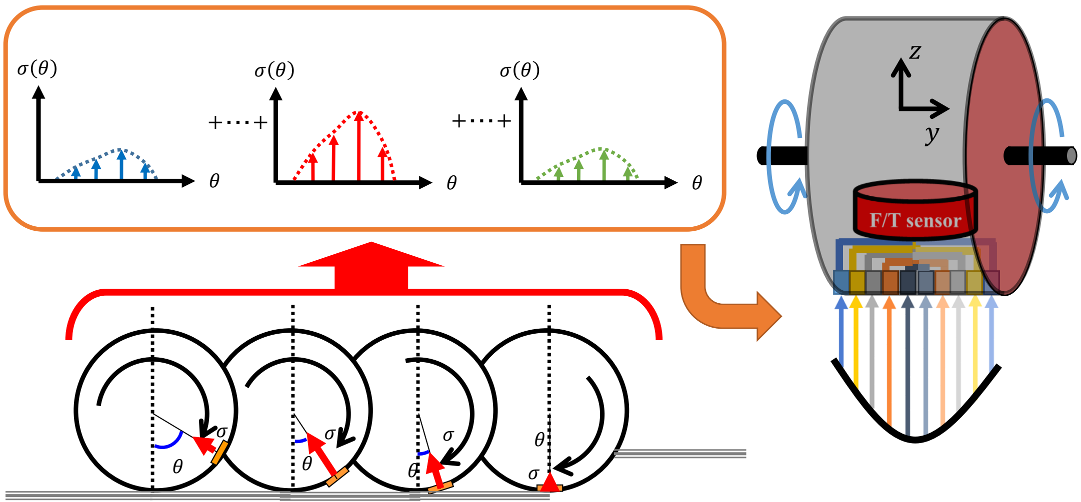

Fig. 5. Measurement Process of 2D Stress Distribution

7. Let the two-wheel rover traverse the sandy slope under a constant condition, and measure the normal stress while the wheel rotates.
8. Measure the stress distribution on an identical slope, and use the average data for three repetitions of the test.
9. Repeat steps 3 to 8 for each contact-part position (Fig. 5).

Using the procedure described above, we obtained stress distributions for 10 locations in the circumferential direction. Then, the 2D stress distribution is obtained by overlapping the obtained stress distributions (Fig. 5).

III. Calibration

In this study, we used two calibration methods for accurately measuring the stress distribution: (1) calibration of the measurement position in the wheel's width direction, and (2) calibration of the contact area between the soil and contact-part. In this section, we describe these two methods.

A. Calibration for Measurement Position

The device used in this study measures the normal force at different positions by changing contact-parts. Each contact-part generates a different moment according to the distance between the wheel center and the contact-part. Therefore, as shown in Fig. 6, we conduct a calibration of the stress measurement for each contact position by using several balance weights. Fig. 7 and Fig. 8 show the measurement results. The measured values near the sides of the wheel were smaller than those near the center of the wheel because of the moment's effect. Therefore, we define the correction coefficient k_{pos} to obtain the actual normal force as follows:

$$k_{pos} = \frac{W_a}{W_m}, \tag{1}$$

where W_a and W_m denote the actual balance weight and detected mass of the measurement device, respectively.

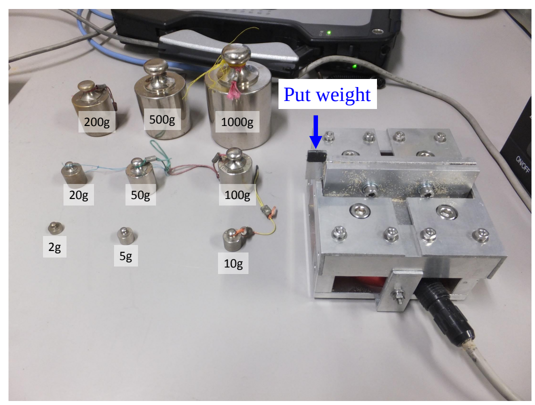

Fig. 6. Calibration for Measurement Point

B. Calibration for Contact Area

In order to expose the contact-part to the wheel surface, the wheel has a hole that is slightly larger than the area of the contact-part. Because soil enter the gap between the wheel surface's hole and the contact area of the measurement device, the contact-part become covered with soil, as shown in Fig. 9. Thus, the soil touches the contact-part over a larger area. Therefore, we introduce the correction coefficient k_{area} for the contact area to precisely evaluate the stress. First, k_{area} must satisfy the following condition:

$$1 < k_{area} < \frac{A_h}{A_c} \tag{2}$$

where A_h is the area of the hole used to expose the contact-part, and A_c is the area of the contact-part. In our case, A_c is 2.4mm $\times$ 10.4mm. Each hole has a 1-mm gap surrounding the contact-part. Therefore, A_h is 4.4mm $\times$ 12.4mm. In this study, we experimentally obtained $k_{area} = 1.6$ to balance the vehicle's weight.

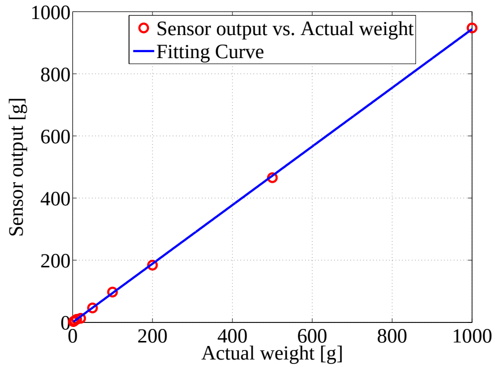

Fig. 7. Calibration Near Center of Wheel

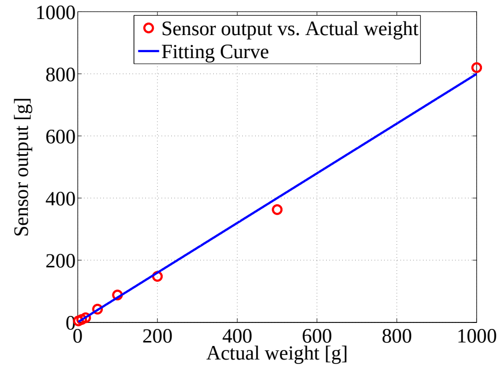

Fig. 8. Calibration Near Side of Wheel

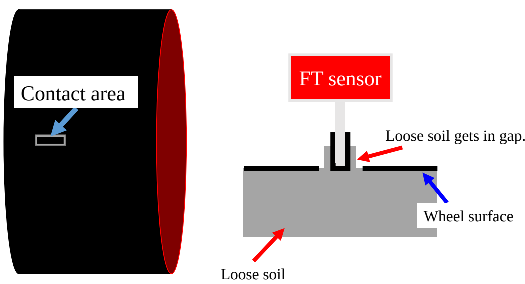

Fig. 9. Illustration of Contact Area

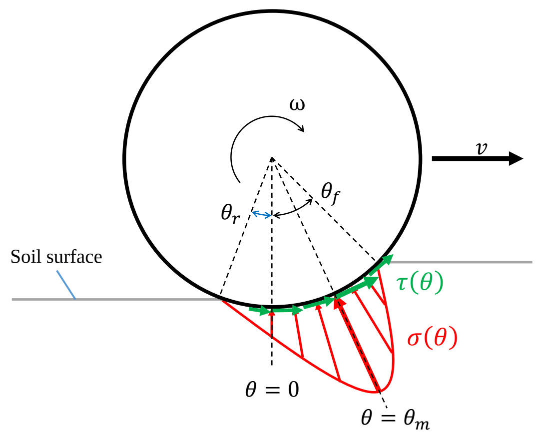

Fig. 11. Illustration of Normal Stress and Shear Stress Distribution generated beneath a Wheel

IV. Results and Discussions

Fig. 10(a) shows the measurement results for the 2D stress distribution when the test bed travels on flat loose soil, and Fig. 10(b), (c), and (d) show the measurement results for the 2D stress distribution when the two-wheel rover test bed traverses a slope.

When the rover traverses flat loose soil (Fig. 10(a)), the wheel's entry angle and departure angle are uniform over the wheel's width, and the peak of the stress is generated at almost the center of the wheel. On the other hand, when the rover laterally traverses a loose soil slope (Fig. 10(b), (c), and (d)), although the departure angles are almost the same over the wheel's width, the entry angles are different at the upper side and lower side of the slope. The stress is generated on one portion of the slope. Furthermore, the peak of the stress moves from the wheel's center to the slope side.

We found that this is caused by the difference in wheel sinkage between the left side and right side of the wheel. When the rover traverses a loose soil slope with the wheel inclined toward the slope, the sinkage on the upper side of the slope increases. Thus, the entry angle to the soil on the upper side of the slope becomes larger. On the other side, the entry angle to the soil on the lower side of the slope becomes smaller because the sinkage on the lower side of the slope decreases. Based on the above, we found that the peak position of the normal stress is shifted to the upper side of the slope.

On the other hand, when a rover traverses a loose soil slope, sideslip occurs because of the slope failure caused by the rotating wheel. We found that the sideslip on the lower side of a slope is caused by pushing aside the soil located in the forward portion of the wheel.

V. Evaluation of Measurement Results

In order to evaluate the validity of the measured 2D normal stress distribution, we examine whether the weight of the two-wheel test bed is balanced using the summation of the vertical components of the normal stress $\sigma(\theta)$ and shear stress $\tau(\theta)$ generated beneath the wheel as shown in Fig. 11. The normal force of the wheel can be calculated using the following equation:

$$W = r \int_{-b/2}^{b/2} \int_{\theta_r}^{\theta_f} \{\tau(\theta) \sin\theta + \sigma(\theta)\cos\theta\} d\theta dy, \quad (3)$$

where r is the wheel radius, b is the wheel width, θ_f is the entry angle into the soil, θ_r is the departure angle from the soil, and θ is the rotational angle of the wheel.

In this study, the normal stress $\sigma(\theta)$ is measured, and the shear stress $\tau(\theta)$ is calculated by the following equation [10]:

$$\tau(\theta) = (c + \sigma(\theta)\tan\phi)\left[1 - e^{-j_x(\theta)/k_x}\right], \quad (4)$$

where c is the cohesion, ϕ is the internal friction angle of the soil, and k_x is the shear deformation parameter. j_x is

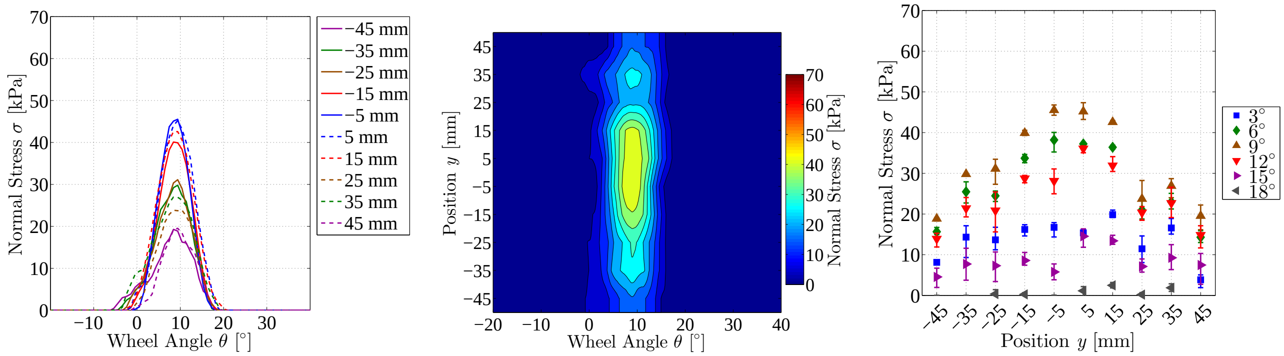

(a) Slope angle $\alpha = 0°$

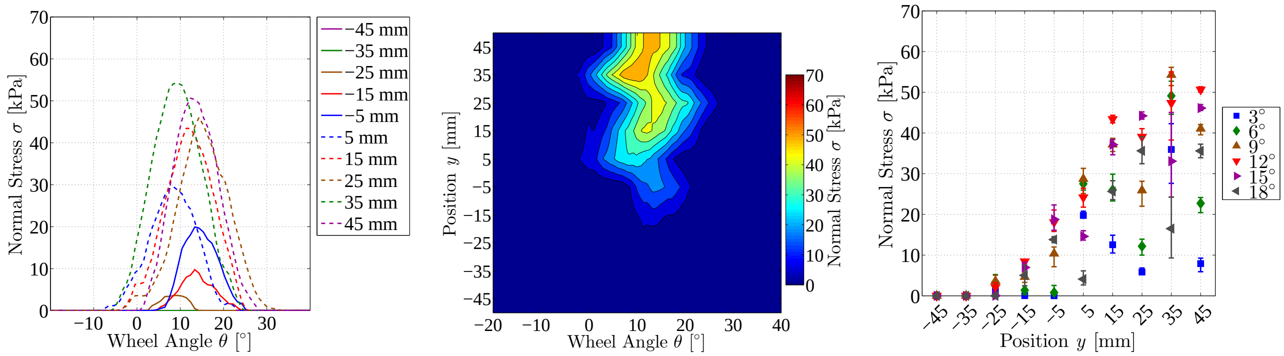

(b) Slope angle $\alpha = 10°$

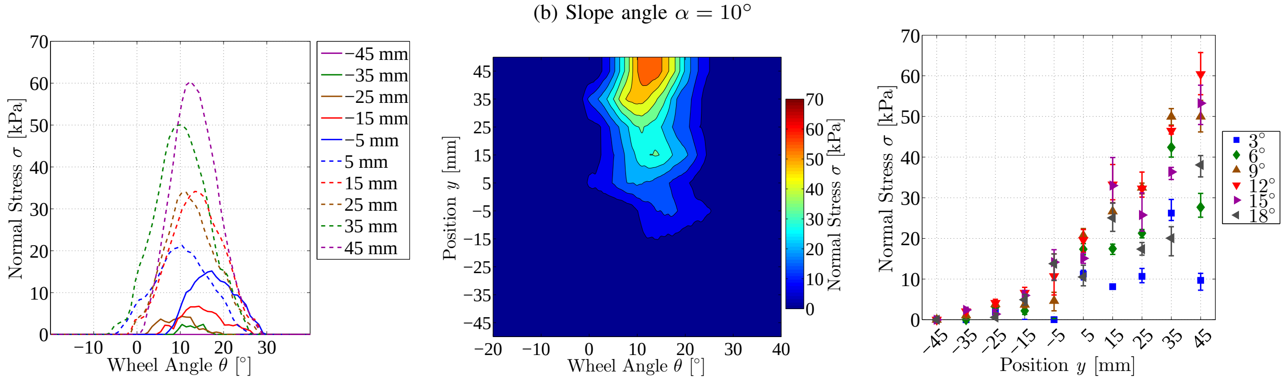

(c) Slope angle $\alpha = 15°$

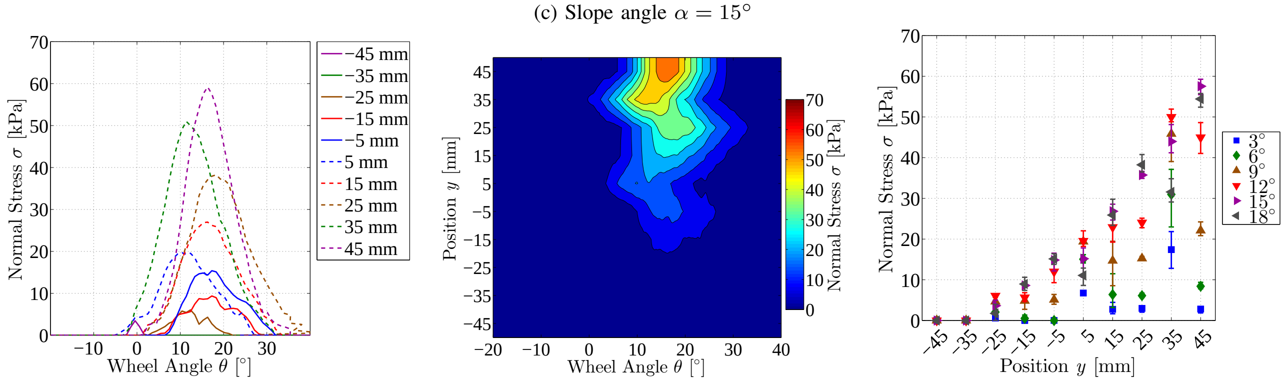

(d) Slope angle $\alpha = 20°$

Fig. 10. Measurement Results; The graphs in the left column show the normal stress distribution in circumferential direction of a wheel; The graphs in the middle column show contour plot of 2D normal stress distribution of a wheel; The graphs in the right column show the normal stress distribution in the width direction of a wheel.

the soil's shear displacement that develops along the contact area between the wheel and soil and is defined by the slip velocity v_s of the soil.

The slip velocity v_s of the soil is defined by the difference between the circumferential speed $r\omega$ and the tangential component of the traveling speed of a wheel and is expressed by the following equation:

$$v_s = r\omega - v\cos\theta = r\omega\{1-(1-s)\cos\theta\}, \tag{5}$$

where s is the slip ratio. The slip ratio is expressed as follows:

$$s = 1 - \frac{v_x}{r\omega} \tag{6}$$

where v_x is the traveling speed of the two-wheel test bed. Based on equation (5), the shear displacement j_x generated along the contact area between the wheel and soil is calculated using the following equation:

$$\begin{aligned} j_x &= \int_0^t v_s dt = \int_\theta^{\theta_f} r\omega\{1-(1-s)\cos\theta\}\frac{d\theta}{\omega} \\ &= r\{\theta_f - \theta - (1-s)(\sin\theta_f - \sin\theta)\}, \end{aligned} \tag{7}$$

where the shear stress is calculated from the measured normal stress distribution and the parameters listed in Table II.

A. Evaluation Method

When the two-wheel robot traverses a loose soil slope, we assume that the weight acting on the front wheel and that on the rear wheel are the same. Therefore, the estimated weight $W_{est}$of the test bed is calculated as follows:

$$W_{est} = 2\frac{F_{z_r}}{g}, \tag{8}$$

where F_{z_r} denotes the normal force estimated from the 2D stress distribution of the rear wheel, and g denotes the acceleration of gravity. The error W_E between the actual weight of the vehicle and estimated weight of the test bed is defined by the following equation:

$$W_E = \left(1 - \frac{W_{est}}{W_{act}}\right) \times 100, \tag{9}$$

where W_{act} is the actual weight of the vehicle.

TABLE II

TERRAIN PARAMETERS TRAVERSING LOOSE SOIL SLOPES.

Parameter	Value	Unit	Source
c	0	kPa	[11]
ϕ	38	°	[11]
k_x	0.03	m	[11]
s	0.06	-	Experiment
θ_f	33($\alpha = 10°$)	°	Experiment
θ_r	-8($\alpha = 10°$)	°	Experiment
θ_f	30($\alpha = 15°$)	°	Experiment
θ_r	-7($\alpha = 15°$)	°	Experiment
θ_f	40($\alpha = 20°$)	°	Experiment
θ_r	-5($\alpha = 20°$)	°	Experiment

TABLE III

ACTUAL WEIGHT VS. ESTIMATED WEIGHT TRAVERSING LOOSE SOIL SLOPES

Slope angle [°]	Actual weight [kg]	Estimated weight [kg]	Error [%]
0	14.8	14.6	+1.4
10	14.8	15.4	-3.9
15	14.8	14.3	+3.5
20	14.8	15.3	-3.3

B. Evaluation Result

We evaluated the obtained normal stress distribution based on the above method. Table III lists the actual vehicle weight, estimated vehicle weight, and the error between for each slope inclination angle.

According to the results, the error between the actual vehicle weight and estimated weight under each slope inclination angle was less than $\pm 5\%$.

VI. CONCLUSIONS

In this paper, we described a measurement method for the 2D stress distribution of a wheel, particularly in a case where a rover laterally traverses a loose soil slope with a wheel inclined in the slope direction. We experimentally obtained 2D stress distribution, and the error between the actual weight and estimated weight was less than 5%. In addition, we clarified that the peak of the normal stress distribution generated beneath a wheel was offset from the center of the wheel to the slope portion when the rover traversed a loose soil slope with the wheels inclined toward the slope.

For future work, a stress distribution model for a wheeled robot is needed. This could be used to estimate side slippage.

REFERENCES

[1] M. G. Bekker, *Theory of Land Locomotion*. Ann Arbor, MI: The University of Michigan Press, 1956.

[2] J. Y. Wong, *Theory of Ground Vehicles*, 4th ed. Hoboken, New Jersey: John Wiley & Sons, Inc., 2008.

[3] G. Ishigami, A. Miwa, K. Nagatani, and K. Yoshida, "Terramechanics-based model for steering maneuver of planetary exploration rovers on loose soil," *Journal of Field Robotics*, vol. 24, no. 3, pp. 233–250, Mar. 2007.

[4] E. Hegedus, "Pressure distribution and slip-sinkage relationship under driven rigid wheels," Army Tank Automotive Center, Warren, MI, Land Locomotion Lab, Tech. Rep., 1963.

[5] G. Krick, "Radial and shear stress distribution under rigid wheels and pneumatic tires operating on yielding soils with consideration of tire deformation," *Journal of Terramechanics*, vol. 6, no. 3, pp. 73–98, 1969.

[6] K. Nagatani, A. Ikeda, K. Sato, and K. Yoshida, "Accurate estimation of drawbar pull of wheeled mobile robots traversing sandy terrain using built-in force sensor array wheel," in *Proceedings of the 2009 IEEE/RSJ International Conference on Intelligent Robots and Systems*, St. Louis, MO, USA, Oct. 2009, pp. 2373–2378.

[7] C. Senatore and K. Iagnemma, "Analysis of stress distributions under lightweight wheeled vehicles," *Journal of Terramechanics*, vol. 51, pp. 1–17, Feb. 2014.

[8] T. Shirai and G. Ishigami, "Accurate Estimation of Wheel Pressure-Sinkage Traits on Sandy Terrain using In-Wheel Sensor System," in *Proceedings of the 12th International Symposium on Artificial Intelligence, Robotics and Automation in Space*, no. 8a–3, June 2014.

[9] H. Inotsume, M. Sutoh, K. Nagaoka, K. Nagatani, and K. Yoshida, "Modeling, analysis, and control of an actively reconfigurable planetary rover for traversing slopes covered with loose soil," *Journal of Field Robotics*, vol. 30, no. 6, pp. 875–896, Nov. 2013. [Online]. Available: http://doi.wiley.com/10.1002/rob.21479

[10] Z. Janosi and B. Hanamoto, "The analytical determination of drawbar pull as a function of slip for tracked vehicles in deformable soils," in *Proceedings of the 1st International Conference on Terrain-Vehicle Systems*, Turin, Italy, 1961, pp. 707–736.

[11] M. Sutoh, J. Yusa, T. Ito, K. Nagatani, and K. Yoshida, "Traveling performance evaluation of planetary rovers on loose soil," *Journal of Field Robotics*, vol. 29, no. 4, pp. 648–662, July 2012.